# Effective stress coefficient in shales and its applicability to Eaton's equation

RITUPARNA SARKER and MIKE BATZLE, Colorado School of Mines, Golden, USA

Pore pressure within formations determines the mud weight required to build a balancing fluid pressure downhole. An improper understanding of the subsurface geology and the formation pressures may result in fracturing the formation if the mud weight is too high. In contrast, if mud weight is too low, then formation fluids can flow into the well, potentially leading to well blowouts if not controlled. Complex geological settings make pore-pressure prediction difficult and often inaccurate due to uncertainty in pressure-generating mechanisms. Estimation of proper pore pressures is necessary for designing stable holes and an optimized casing program. In exploration, knowledge of pore pressures can assist in assessing seal effectiveness and in high-grading reservoir sweet spots. It also provides useful calibration information for basin modeling. Hence, it becomes very important to accurately predict pore pressures.

Predicting in-situ reservoir and formation pore pressures from seismic velocity, sonic velocity, and resistivity is a general practice within the industry. The relationship between velocity and pore pressure is controlled by effective stress $P_{eff}$,

$$V = f(P_{eff},.....), \qquad (1)$$

$$P_{eff} = OB - nP_P \qquad (2)$$

where $OB$ is the overburden or the vertical stress, usually obtained by integrating the density log, $P_P$ is the pore pressure, $P_{eff}$ is the effective stress, and $n$ is defined as the effective stress coefficient.

Hence, in order to determine subsurface pore pressure from properties like velocity, determination of $n$ is a must. The typical method of determining $n$ for rocks is through laboratory measurements. Little experimental work has been done on shales, where most instances of overpressure occur. Most models used in velocity-to-pressure transforms are calibrated for sandstone but not for shale.

Overpressure is one of the primary concerns of explorationists, and drilling through overpressured shale is still considered a hazard, both in terms of personnel safety and well economics. The causes of overpressure generation have been attributed to undercompaction, fluid expansion, lateral transfer, and tectonic loading (Bowers, 2002). In tectonically relaxed environments, shale compaction can be related to effective stress (Tosaya, 1982; Bowers 2002). The relationship is mainly controlled by the stress history of the rock, i.e., whether or not the rock has experienced higher effective
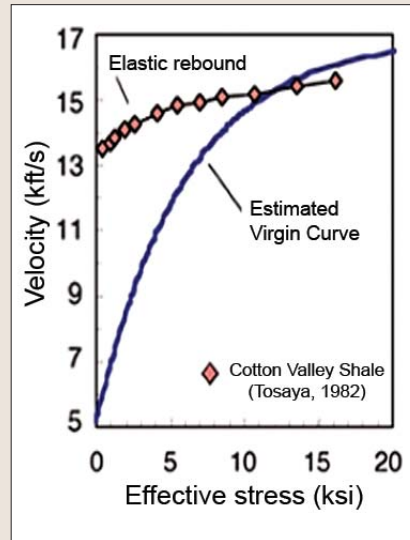


**Figure 1.** $V_P$ data on rebound behavior for Cotton Valley shale, showing virgin and unloading cases. $V_P$ changes are much more pronounced for the loading case compared to the unloading case. This change in the nature of the velocity path is also termed "velocity hysteresis." Note the virgin curve is an estimated curve for normal compaction behavior of shales (adapted from Bowers, 2002).
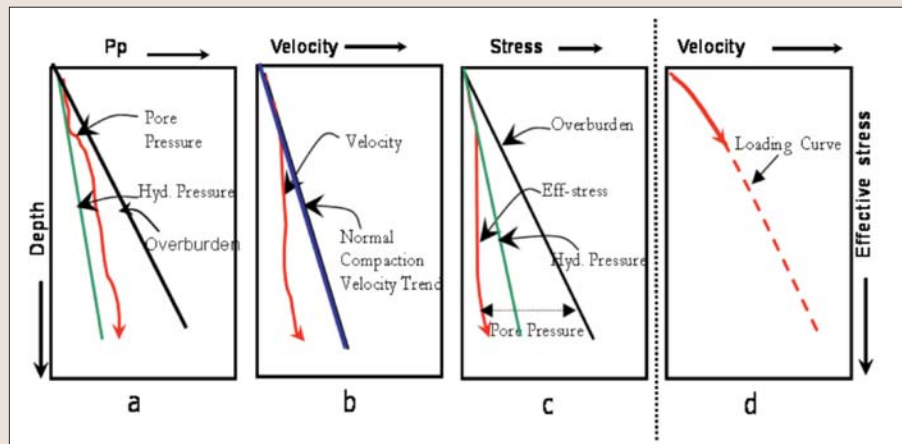


**Figure 2.** Schematic showing a case when overpressure is caused by undercompaction (a Gulf of Mexico case). The directions of arrows on the red curves indicate the direction of increasing confining stress (modified from Bowers, 1995).
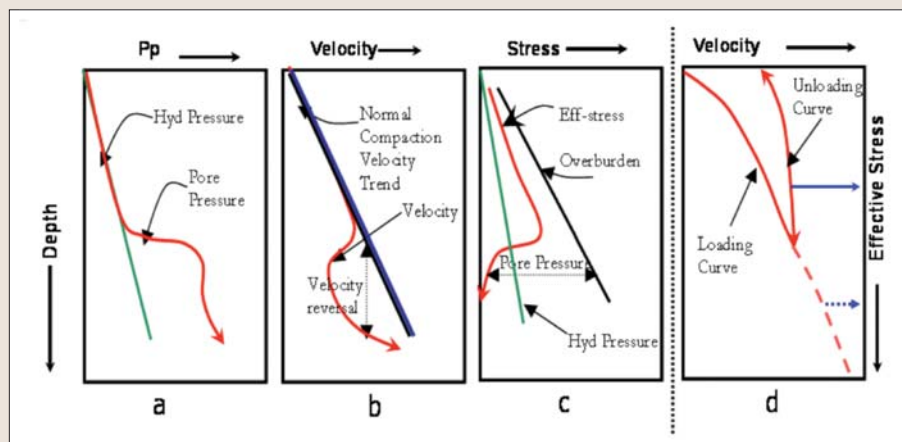


**Figure 3.** Schematic showing a case when cause of overpressure is fluid expansion. Loading curve overestimates effective stress and underestimates $P_P$. The directions of arrows on the red curves indicate the direction of increasing confining stress (modified from Bowers 1995).

stress than its current stress state (whether the rock has been unloaded after deeper burial).

Recent clay-rich sediments that are deposited on the seafloor are unconsolidated and have very high porosity (around 80%, according to Bowers). Hence, sonic velocities at the seafloor are very close to the P-wave velocity of water. As these sediments are buried, mechanical compaction occurs under increasing effective stress, increasing vertical load, and hydrostatically increasing pore pressure. The sediments lose porosity, while sonic velocity and density increase, ultimately approaching a limit beyond which there is no further change in rock properties. This increasingly effective stress path with associated rock properties is called a virgin compaction curve if the pore pressure increases hydrostatically. A similar term used in experimental rock-physics experiments is a "loading curve" that indicates changing rock properties for compacting sediments under uniformly increasing effective stress conditions.

During the compaction process, the rock may see a state where the effective stress is reduced. Compaction is predominantly an inelastic process; however, effective stress reduction results in elastic rebound alone, leading to a different unloading curve. Instead of following a virgin curve, the rock then follows a flatter path as shown in Figure 1.

Various mechanisms can cause rocks to be overpressured. The most common is compaction-disequilibrium or under-compaction where the increasing overburden stress is counteracted by increased pore pressure as shown by Figure 2. Fluids within the clay-bearing rocks cannot escape due to their very low permeability, and, as a result, the pore pressure increases above hydrostatic pressure as shown in Figure 2a. In such a case, the rock deviates from the normal compaction trend or the virgin curve, and the velocities measured are lower than expected (Figure 2b). The effective stress that controls these properties is a function of the difference between the overburden and pore pressure. Instead of increasing uniformly, overpressure zones follow a path where the rate of increase is reduced or follow a constant effective stress path as shown in Figure 2c. Hence, the actual loading stops at that point where effective stress stops increasing (Figure 2d).

Undercompaction itself cannot cause the effective stress to decrease (Bowers, 1995), i.e., the rock does not see a velocity hysteresis and hence does not follow an unloading curve. Instead, its effective stress state can become constant with increasing depth. However, if the cause of overpressure is fluid expansion, then the pore pressure will increase at a faster rate than overburden stress as shown by Figure 3a. In this case, the effective stress decreases as burial continues (Figure 3c). The lowering of effective stress makes the rock deviate from the loading curve; i.e., a velocity reversal occurs in the rock (Figure 3b). The velocities inside the reversal zone track a slower trend. This figure explains the importance of understanding the cause of overpressure when estimating pore pressures from velocity data. Not understanding the velocity hysteresis could lead to wrong estimations of effective stress and thus pore pressures, as indicated in Figure 3d. If the cause of overpressure generation is not well understood, then the loading curve could lead to erroneous estimation of the effective stress state of the rock. The loading curve would overestimate the effective stress (the dashed blue arrow in Figure 3d) when the actual stress state of the rock is on the unloading curve marked with the solid blue arrow. This overestimation of effective stress causes the pore pressure to be underestimated, and an incorrect prediction of mud weight would result. This velocity hysteresis in the rock can be quantified with an effective stress coefficient $n$. $n$ scales the influence of changes in pore pressure and thus establishes the right
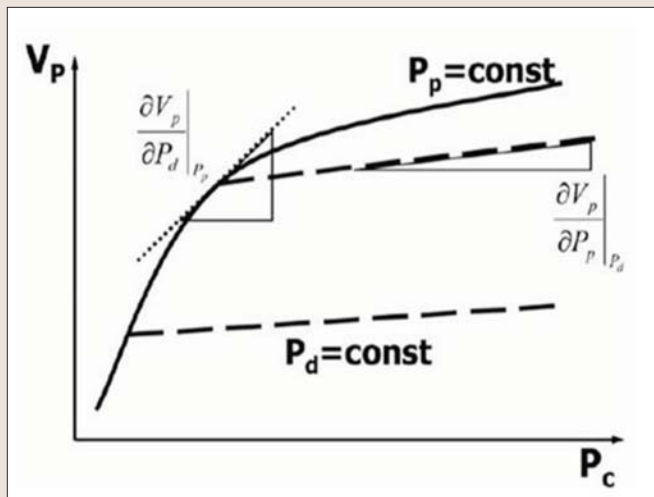


**Figure 4.** Schematic showing calculation of n using Equation 6.
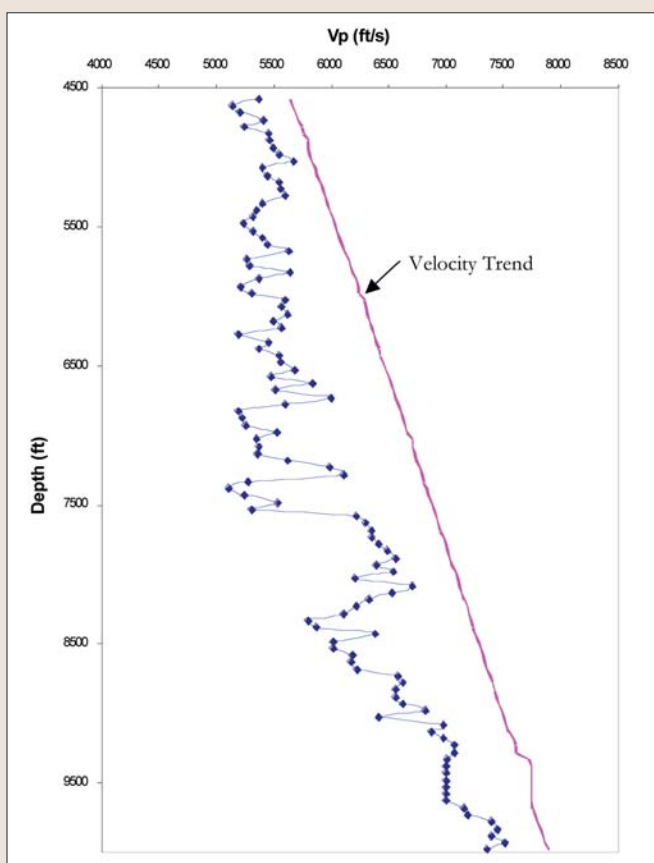


**Figure 5.** Picked shale sonic $V_P$ (blue) and normal compaction trend line for a North Sea well (red) plotted as a function of depth. Normal compaction trend established using the 1989 equation of Eberhart-Phillips et al.

velocity-to-effective stress relationship for prediction of accurate pore pressures.

**Estimation of $n$.** Estimation of $n$ can be performed from laboratory-measured velocity as a function of effective stress. Experimental studies performed previously have demonstrated that porosity of compacting sediments is a function of differential pressure (Terzaghi, 1936).

$$P_{diff} = P_C - P_P \qquad (3)$$

| $n$ range for $V_P$ | $n$ range for $V_s$ | Lithology | Reference |
|---|---|---|---|
| 1 | — | Sandstone | Wyllie et al., 1958 |
| Greater than 1 | Greater than 1 | Sandstone | King, 1996 |
| 0.9–0.5 | — | Granite | Todd and Simmons, 1972 |
| 0.99–0.84 | 1.02–1.17 | Sandstone | Christensen and Wang, 1985 |
| 0.95–0.88 | 1–1.1 | Sandstone | Hornby, 1996 |
| 0.87–0.5 | 1–0.88 | Shale | Hornby, 1996 |
| 0.93–0.615 | – | Sandstone | Prasad and Manghnani, 1997 |

**Table 1. "n" ranges estimated from ultrasonic velocities previously by various researchers.**
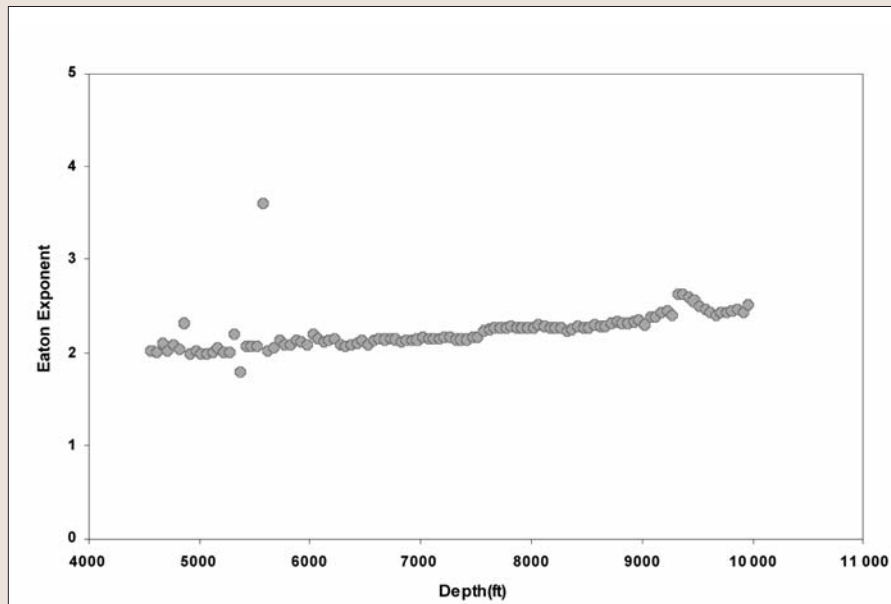


**Figure 6.** *Calculated Eaton P-wave exponent (E value) for North Sea well. Gray circles correspond to E computed using assumption n=1.*

Theoretical analysis by Biot and Willis (1957) indicated that velocity is dependent on effective pressure $P_{eff}$ as

$$P_{eff} = P_C - nP_P \qquad (4)$$

Here $n$ is defined as the coefficient of internal deformation, which may be less than unity. Later work by Nur and Byerlee (1971) also supported a similar definition of effective stress.

Biot and Willis defined coefficient $\beta$ as the ratio of static pore-space deformation to total bulk-volume change and is given by

$$\beta = 1 - \frac{K_{dry}}{K_m} \qquad (5)$$

where the bulk modulus of dry porous rock is $K_{dry}$ and $K_m$ is the bulk modulus of the solid material. This equation sug-

gests that at shallower depths where $K_{dry} << K_m$, $n \approx 1$; hence, Equation 4 reduces to the commonly used expression given by Equation 3. However, Equation 5 is not applicable to dynamic measurements (like ultrasonic, sonic, or seismic frequencies). It holds only for static measurements. Todd and Simmons in 1972 defined $n$ for dynamic measurements. This is one of the most popular methods for determining $n$ under laboratory conditions and holds true for dynamic rock properties.

$$n = 1 - \frac{\left(\partial Q / \partial P_p\right)_{P_d}}{\left(\partial Q / \partial P_d\right)_{P_p}} \qquad (6)$$

where Q = any measured physical property, $P_P$ = pore pressure, and $P_d$ = differential pressure. A graphical representation of Equation 6 is shown schematically in Figure 4.

A tabulation of experimentally obtained $n$ values for different kinds of lithology is shown in Table 1. Extensive work has been done to determine $n$ for sandstones but little experimental work has been done on shales. Experimental work by Hornby (1996) suggests that $n$ for shales varies as a function of differential pressure and varies from lithology to lithology. He also indicated that $n$ varies as a function of the mode of elastic-wave propagation.

**Applicability of $n$.** Eaton's algorithm (Eaton, 1975) is one of the most popular methods for pore-pressure prediction. It estimates the pore pressure from the seismic P-wave velocity, $V_{obs}$ using Equation 7.

$$\frac{P_P}{D} = \frac{P_c}{D} - \left(\frac{P_c}{D} - \frac{P_P}{D_n}\right)\left(\frac{V_{obs}}{V_n}\right)^E \qquad (7)$$

where $P_P/D$ is the predicted formation pore-pressure gradient in psi/ft; $P_C/D$ is the overburden stress gradient in psi/ft; $P_P/D_n$ is the normal static pore-pressure gradient, usually taken as 0.465 psi/ft; $V_n$ is the normal compaction trend velocity for shales, and $V_{obs}$ is the observed shale velocity. E is the Eaton exponent.

Ebrom (2003) states that Eaton's method may not be the most accurate method for complex geological settings, but it is often used as a standard against which all other pressure prediction models are compared. Although the algorithm claims to be an effective stress approach to computing pore pressure from velocity, it does not actually use effective stress in its true sense. The assumption in Eaton's equation is that $n = 1$ and $P_{eff} = P_C - P_P$. This approach might be true for some Gulf of Mexico wells for which the equation had actually been derived, but may not hold true for wells from locations where the cause of overpressure generation is not compaction disequilibrium.

Eaton's exponent $E$ is a measure of the sensitivity of the
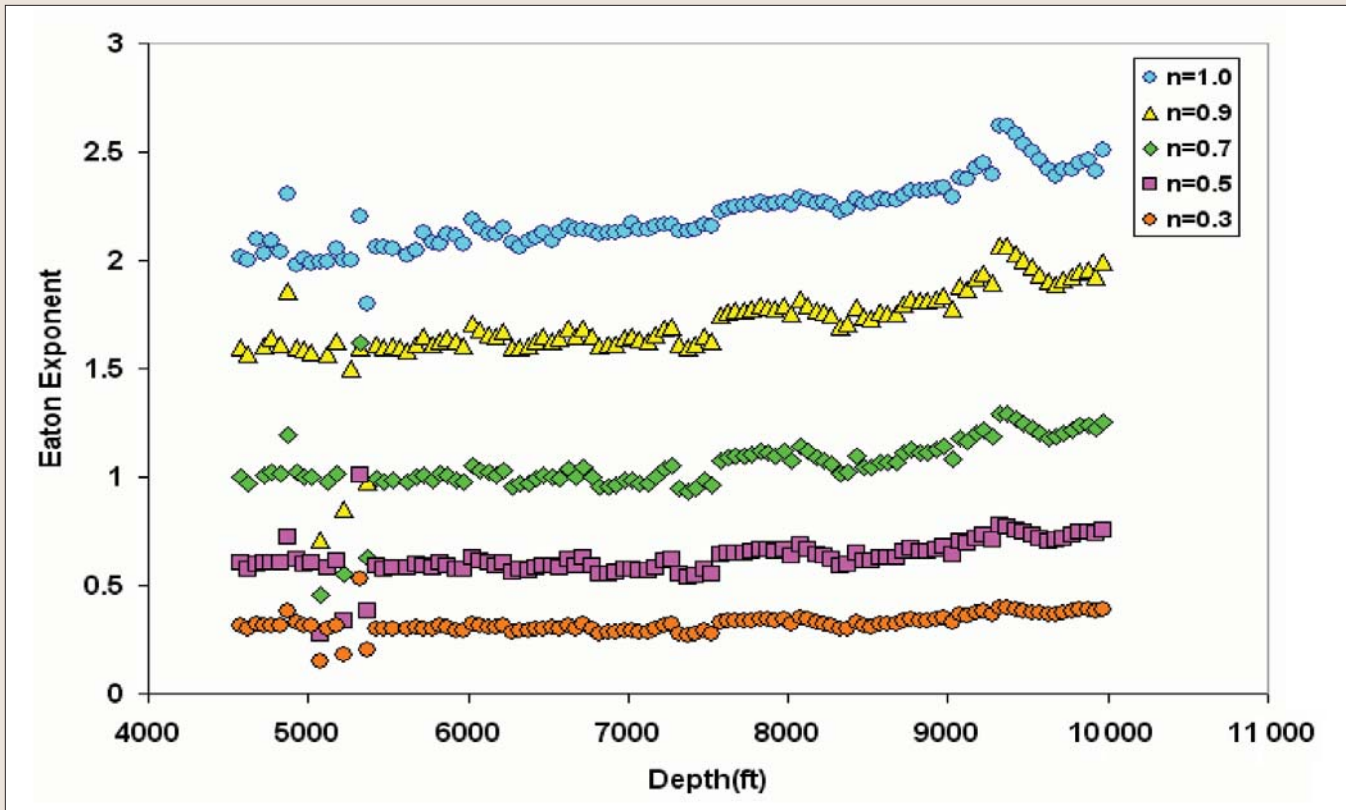
*Figure 7. Sensitivity of E to n. The colored curves indicate the sensitivity of "E" to change in n. Note that velocities are most sensitive to pore pressure at n=0.7, i.e., when E = 1.*

sonic velocities to effective stress (Ebrom, 2003). For most cases in the Gulf of Mexico, an Eaton exponent of 3 for P-wave velocities and 2 for S-wave velocities is appropriate (Ebrom, 2003). A larger value of *E* indicates insensitivity of the velocities to changes in effective stress. However, a single value of *E* is often insufficient to predict pore pressures for the entire section, and this number needs to be varied with depth depending on the degree of overpressure in the subsurface. However, if a depth-varying *n* is used instead in the equation, it serves the same purpose and has more physical significance. In this way, the Eaton equation can be extended to areas where there is significant overpressure due to other causes. We thus try to modify the equation by including the effective stress coefficient.

$$\frac{P_P}{D} = \frac{1}{n}\left\{\frac{P_c}{D} - \left(\frac{P_c}{D} - n\frac{P_P}{D_n}\right)\left(\frac{V_{obs}}{V_n}\right)^E\right\} \quad (8)$$

To model the Eaton's exponent, we rearrange Equation 8 with the assumption that *n*=1 for normally compacting sediments.

$$E = \frac{\log\left(\frac{\dfrac{P_C}{D} - n\dfrac{P}{D_{obs}}}{\dfrac{P_C}{D} - \dfrac{P}{D_n}}\right)}{\log\left(\dfrac{V_{obs}}{V_n}\right)} \quad (9)$$

We do the analysis on an overpressured well from the Norwegian sector of the North Sea. For modeling the pore

pressure, we use sonic velocity to compute pore pressure using already published models, and then finally calibrate the results using mud weight information for the well under consideration. MDT pressures are measured in sands and may not be an accurate representation of shale pressures. Hence, we use the surface mud weight only for shale pressures (although these weights are an interpretation of the pressure by the on-site mud engineer). In order to establish a normal compaction trend line, we resort to an iterative process where we use different kinds of models with varying parameters and then try and obtain a match with the final pressure information from the well. We also try to match the predicted compaction trend to the shallow, normally compacted sediments in other wells from the same area. We used the equation from Eberhart–Phillips et al., often referred to as the EHZ equation, to establish a normal compaction trend (shown in Figure 5). Various other previously published normal compaction trends for shales in this area were also evaluated. However, the best match was obtained using the approach stated above. The density log was integrated to establish an overburden gradient. Once the pore pressure and the trend line were established, *E* was back-calculated using Equation 7.

The modeled *E* computed using the differential pressure approach is shown in Figure 6. In order to run a sensitivity analysis on *n*, we vary *n* between .3 and 1. *E* in Eaton's equation is a fitting parameter and needs to be changed in order to obtain a good match between $V_{obs}/V_n$ and $\sigma_{obs}/\sigma_n$, where $\sigma_{obs}$ and $\sigma_n$ are the observed effective stress and normal effective stress, respectively. Velocities are most sensitive to pressures when *E*=1. We believe that when we use effective stress, the velocity and pressure have a one-to-one relationship and need no exponent to enhance or diminish the
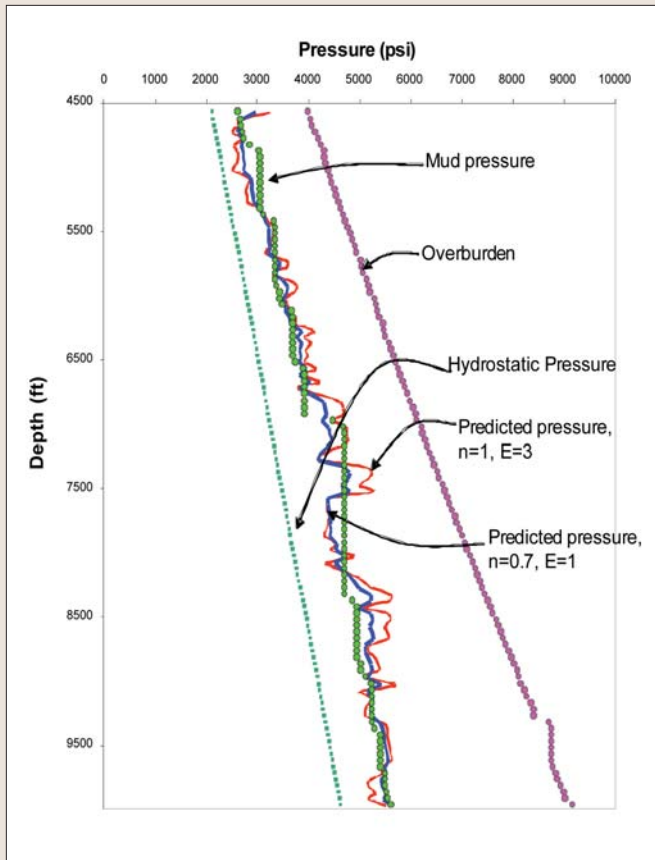
***Figure 8.*** *Comparison of surface mud weights with predicted pressure using Eaton's equation with n=1, E=3 and E=1, n=0.7. The effective stress approach reduces rms error by at least 15%.*

velocity response. Hence, instead of using the fitting parameter *E*, we modify Eaton's equation with *n*, which is a rock property. With this effective stress approach, Eaton's equation can be extended to pore-pressure prediction from seismic velocities as well.

Therefore, from Figure 7 we can say that for this well *n* = .7 would be a good approximation. However, to obtain a more rigorous pressure transform, a depth-varying *n* should be used. This could be obtained by back-calculating *n* from Equation 7 from a calibration well where pressure measurements are available.

We do a comparison of the actual mud weight in the well with the pressures predicted using Eaton's equation both with the differential pressure approach and the effective stress approach. An rms error calculated for both cases shows that the effective stress approach reduces error in pressure prediction by 15%. Figure 8 shows the comparison. It should be noted here that velocity data from the shallow section are missing. Hence, we cannot make a conclusion about the cause of overpressure for this well from the velocity and normal compaction trend, specifically. However, an analysis of other wells from the same area and also published literature indicate that the overpressure in the Miocene section is mainly due to unloading (mainly smectite-to-illite transition). Plots of $V_P$ versus differential pressure (Figure 9) and $V_P$ versus effective stress (Figure 10) for the well under consideration are provided for comparison. Effective stress is computed using a depth-varying *n* in Figure 10. Close analyses of the two plots indicate that the cause of overpressure generation is unloading. With the effective stress approach, we see that with increasing effective stress, $V_P$ increases, whereas in Figure 9 we see that velocity and differential pressure do not show any particular trend.
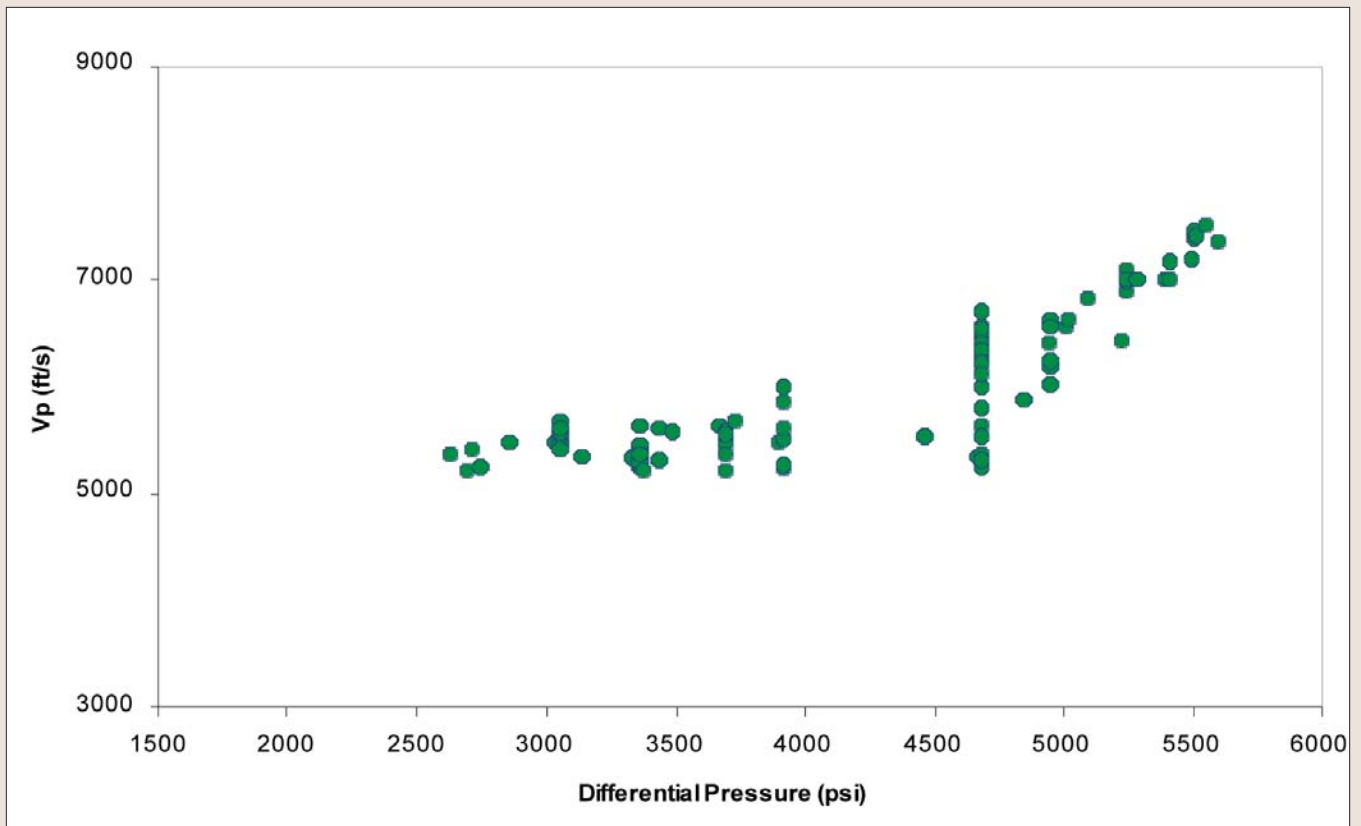


***Figure 9.*** *Plot of $V_P$ versus differential pressure ($P_C - P_P$).*
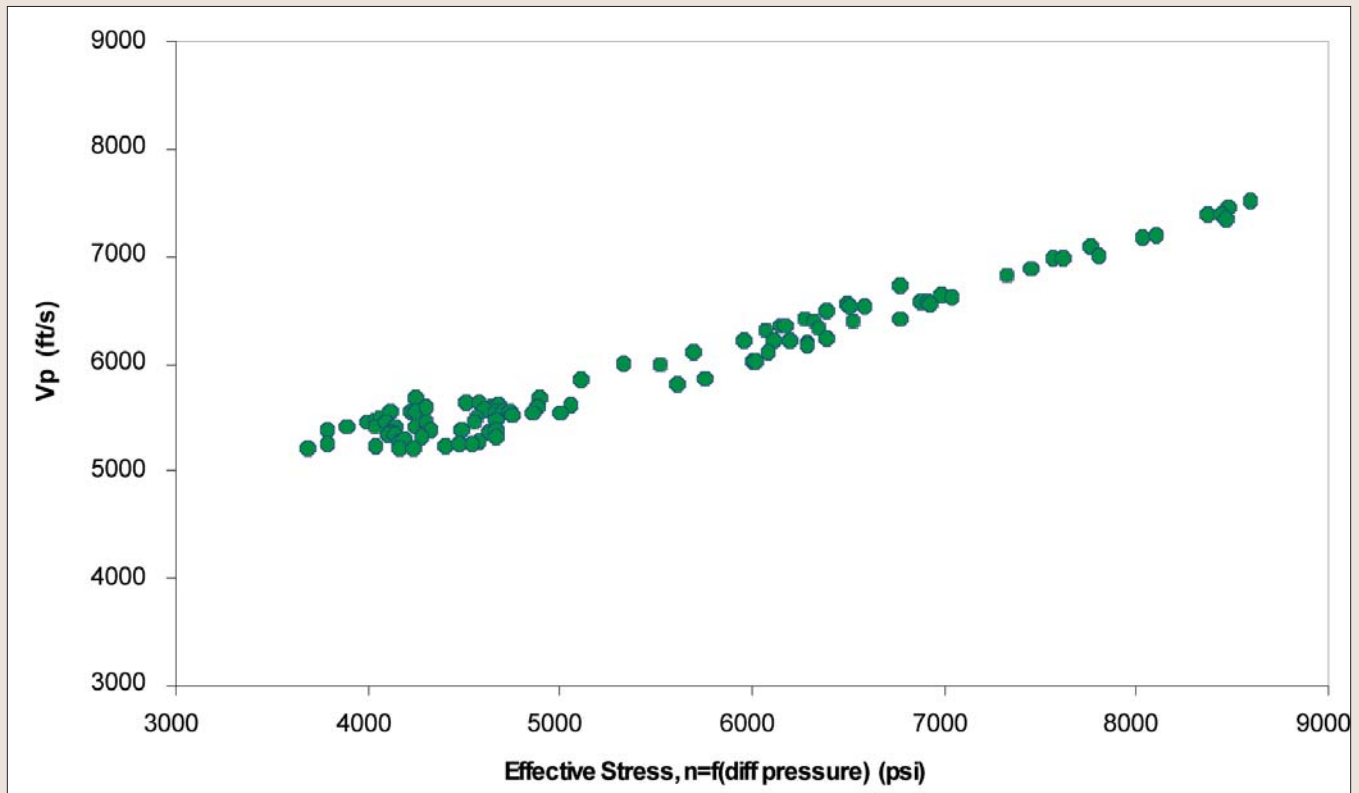
**Figure 10.** Plot of $V_P$ versus effective stress ($P_C$ -$nP_P$). $V_P$ increases with increasing effective stress.

**Discussion.** An effective stress approach to Eaton's equation shows that an *n* value of around .7 is enough to model actual pore pressure from sonic velocities for the North Sea well with an Eaton exponent of 1. This approach improves the accuracy of estimating pore pressures from sonic velocities by at least 15% when compared to using a constant Eaton's exponent of 3. From the analysis, we understand that the effective stress coefficient is a very important parameter in pore-pressure prediction, and if the coefficient is known, Eaton's equation can be used successfully in areas with complex geological settings. More direct laboratory measurements are required for shales, which compose almost 75% of the subsurface sedimentary rocks.

**Suggested reading.** "An experimental investigation of effective stress principles for sedimentary rocks" by Hornby (SEG *Expanded Abstracts*, 1996). "Pore pressure estimation from velocity data: Accounting for pore pressure mechanisms besides under compaction" by Bowers (*SPE Drilling and Completion*, 1995). "Pore-pressure prediction from S-wave, C-wave, and P-wave velocities" by Ebrom et al. (SEG *Expanded Abstracts*, 2003). "Detecting high overpressure" by Bowers (*TLE*, 2002). "The equation for geopressure prediction from well logs" by Eaton (*Society of Petroleum Engineers*, 1975). "Empirical relationships among seismic velocity, effective pressure, porosity, and clay content in sandstone" by Eberhart-Phillips et al. (GEOPHYSICS, 1989). "Pore/fracture pressure determinations in deep water" by Traugott (*World Oil, Deepwater Technology Special Supplement*, 1997). "Velocity-depth trends in Mesozoic and Cenozoic sediments from the Norwegian Shelf" by Storvoll et al. (*AAPG Bulletin*, 2005). TLE

*Corresponding author: rsarker@mines.edu*